HHS Public Access

Author manuscript

Mol Carcinog. Author manuscript; available in PMC 2015 October 01.

Published in final edited form as:

Mol Carcinog. 2015 October ; 54(10): 959–970. doi:10.1002/mc.22165.

Genetic background determines if *Stat5b* suppresses or enhances murine hepatocarcinogenesis

Christopher Oberley, **Andrea Bilger**, and **Norman R. Drinkwater**

McArdle Laboratory for Cancer Research, School of Medicine and Public Health, University of Wisconsin, Madison, Wisconsin, United States of America

Abstract

Murine hepatocarcinogenesis requires growth hormone (GH). To determine if the GH-responsive transcription factor STAT5b (signal transducer and activator of transcription 5b) is also required, we compared the hepatic gene expression profiles of global *Stat5b* null mice to cancer-resistant mice mutant in the GH pathway -- GH-deficient *little* and androgen receptor-null *Tfm* males. We found a high degree of overlap among *Tfm*, *little*, and *Stat5b* null males. The liver cancer susceptibility of global *Stat5b* null mice was assessed on three distinct genetic backgrounds: BALB/cJ (BALB), C57BL/6J (B6), and C3H/HeJ (C3H). The effect of *Stat5b* on hepatocarcinogenesis depended on the genetic background. B6 *Stat5b* null congenic males and females developed 2.4 times as many tumors as wild-type (WT) controls ($P < 0.002$) and the tumors were larger ($P < 0.003$). In BALB/c congenics, loss of STAT5b had no effect on either sex. C3H *Stat5b* null congenic males and females were resistant to liver cancer, developing 2.7- and 6-fold fewer tumors, respectively ($P < 0.02$, 0.003). These results provide the first example of a single gene behaving as both oncogene and tumor suppressor in a given tissue, depending only on the endogenous modifier alleles carried by different genetic backgrounds.

Keywords

growth hormone; sex hormones; liver cancer; mouse genetics

INTRODUCTION

Human liver cancer is a significant global health problem. Liver cancer is the fifth most common cancer in men and seventh most common cancer in women [1]. In 2008, it was estimated there were 522,000 cases of liver cancer in men (7.9% of total cancer cases) and 226,000 cases in women (6.5% of total). Liver cancer is the third most common cause of death from cancer worldwide, and it was estimated that 696,000 people died from liver cancer worldwide in 2008. In the United States (US), approximately 90% of liver cancer is hepatocellular carcinoma (HCC), with intrahepatic cholangiocarcinoma accounting for nearly all of the remaining 10% [2,3]. During the three decades from 1975 and 2005, HCC rates tripled in the US [2].

1400 University Ave, Madison WI 53706, Phone: 608-262-7992, Fax: 608-262-2824, drinkwater@oncology.wisc.edu.

In almost all populations examined, the incidence of HCC is higher in men than women, and liver cancer mortality is also higher in men than women in every region of the world [1]. In the US, incidence is approximately 3-fold higher in men than women [2]. Further, HCC is the fastest growing cause of cancer-related death in men in the US [4]. Although the etiology of male-specific sensitivity to liver cancer is largely unknown, laboratory studies with rodents indicate that sex hormones play a key role in the observed sexual dimorphism of HCC incidence.

Male mice are more sensitive to hepatocarcinogenesis than female mice, having higher incidences of both spontaneous liver tumors and liver tumors induced by perinatal treatment with a variety of chemical carcinogens [5–9]. Gonadectomy studies have shown that sex hormones have opposing roles in hepatocarcinogenesis. Castrated male mice have a lower incidence of liver cancer and develop fewer tumors than intact males [6,8,10–12]. In contrast, ovariectomized female mice are more sensitive to hepatocarcinogenesis, developing more liver tumors with greater incidence than intact female mice [6,11–13]. Additionally, castrated male mice and ovariectomized female mice have similar liver tumor incidences [6,12]. Therefore, androgens enhance and ovarian hormones suppress hepatocarcinogenesis. Recent studies have implicated IL-6 signaling [14] and Foxa1/a2 transcriptional regulation [15] in the suppression of liver tumor development in female mice. In males, studies using mice lacking functional androgen receptors, testicular feminization (*Tfm*) mice, have revealed the importance of the androgen receptor in testosterone-mediated promotion of liver tumors [10]. Perinatal N,N-diethylnitrosamine (DEN) treatment resulted in greater than 25-fold more tumors in wild-type male mice than their *Tfm*/Y counterparts or wild-type females. Furthermore, evidence indicates that testosterone-mediated promotion of hepatocarcinogenesis is indirect, that its action occurs upstream of the hepatocyte [10].

An attractive candidate for the secondary, secreted factor that mediates the androgen effect is GH. The temporal pattern of GH release from the anterior pituitary is sexually dimorphic in many species, including rats, mice, and humans [16–19]. The unique period of little or no circulating GH characteristic of the male profile is thought to be key to driving sex-specific hepatic gene expression and is required for expression of male-specific liver genes, such as male-specific cytochrome P450 enzymes (CYPs) [20]. Genome-wide analysis of a large collection of human liver RNA found 1,249 genes exhibiting sex-biased expression, 70% of which were higher in females [21]. Half of the mouse orthologs to these human sex-biased genes also show sex-biased expression in the mouse liver. Of the sex-biased genes common to human and mouse or rat, 75% were shown to be primarily regulated by pituitary GH based on their response to hypophysectomy [22,23].

The *little* mutation spontaneously arose in C57BL/6 mice and is a point mutation in the growth hormone releasing hormone receptor (*Ghrhr*) gene [24–26]. As a consequence of GHRH insensitivity, *little* mice have serum GH levels that are approximately 5% of that of wild-type B6 mice. To further examine the role of GH in sex-specific sensitivity to liver cancer, preweanling, GH-deficient *little* mice were treated with DEN [12]. The *little* mice were remarkably resistant to liver cancer development. Both male and female *little* mice developed fewer tumors than wild-type mice. *Little* male mice developed 36- to 59-fold fewer tumors than B6 wild-type males. *Little* females were also less susceptible to liver

cancer than wild-type B6 females, though to a lesser degree than seen in *little* males, as they developed 11-fold fewer tumors than wild-type females. The effect was even more pronounced on the C3H/HeJ and C57BR/cdJ backgrounds, as congenic males carrying the *little* mutation on these backgrounds developed less than 1% of the number of tumors developed by wild-type males of the same background. Gonadectomy, which dramatically affected hepatocarcinogenesis in wild-type animals, did not significantly affect hepatocarcinogenesis in *little* animals. Together, the results of the *little* tumor studies support the hypothesis that GH is the secondary factor that indirectly mediates the promoting role of testosterone in male mice.

STAT5b is thought to be the master regulator of sex-specific hepatic gene expression in response to the pulsatile plasma GH profile characteristic of males. High levels of tyrosine-phosphorylated STAT5b, the activated form of STAT5b, are detected in liver nuclei from hypophysectomized male rats following a single GH pulse treatment [27]. Furthermore, high levels of active STAT5b are only detected in nuclear extracts from the livers of males, not females [27,28].

Analysis of STAT5b-deficient mice demonstrated the essential role of STAT5b in sexually dimorphic hepatic gene expression [29–31]. Sexual dimorphism of hepatic gene expression is dramatically reduced in global STAT5b knockout male mice. Of the 1,603 mouse genes showing significant sex-biased hepatic expression, 767 of the 850 genes exhibiting male bias (90%) were down-regulated in global STAT5b knockout (STAT5b KO) males [29]. Furthermore, of the 753 female-biased genes, 461 (61%) were up-regulated in global STAT5b knockout males. Thus, the male-specific hepatic gene expression profile requires STAT5b.

We hypothesized that STAT5b is a necessary molecular mediator of male-specific sensitivity to liver cancer. To assess the contribution of STAT5b to male-specific sensitivity, we performed DEN-induced hepatocarcinogenesis studies using global STAT5b KO mice on three distinct genetic backgrounds. To complement our hepatocarcinogenesis studies, we performed whole-genome hepatic gene expression analysis. We compared the hepatic gene expression profiles of STAT5b KO males on the C57BL/6J and BALB/cJ backgrounds with the expression profiles of male mice previously found to be resistant to hepatocarcinogenesis, *Tfm* and *little*. Despite a high degree of similarity in the hepatic gene expression profiles of *Tfm*, *little*, and *Stat5b* null male mice, the genetic background of the mice determined whether STAT5b deficiency enhanced, suppressed, or had no effect on DEN-induced hepatocarcinogenesis.

MATERIALS AND METHODS

Mice

C3H, B6, and BALB inbred strains were obtained from The Jackson Laboratory (Bar Harbor, ME) and bred in our facilities. Two heterozygous male C.129-*Stat5b*^{tm1Hwd}/J mice were also obtained from The Jackson Laboratory (Bar Harbor, ME). This mouse line was originally created by Dr. Helen Davey [31].

To generate C.129-N_6F_2*Stat5b*^{tm1Hwd} mice, founder heterozygous male C.129-*Stat5b*^{tm1Hwd}/J males were further backcrossed one generation to BALB/cJ females. The resulting heterozygous offspring were mated and their offspring were used in the studies. To generate C.129-$N_{11}F_2$*Stat5b*^{tm1Hwd} mice, founder heterozygous male C.129-*Stat5b*^{tm1Hwd}/J males were backcrossed six generations to BALB/cJ females. At N_{11}, the resulting heterozygous offspring were mated and their offspring were used in the studies. To generate B6.129-N_6F_2*Stat5b*^{tm1Hwd} mice, the founder *Stat5b*$^{+/-}$ males were backcrossed six generations to C57BL/6J females. At N_6, the resulting heterozygous offspring were mated and their offspring (B6.129N_6F_2) were used in the studies. To generate C3H N_6 congenics, the founder *Stat5b*$^{+/-}$ males were backcrossed six generations to C3H/HeJ females. At N_6, the resulting heterozygous offspring were mated and their offspring (C3.129N_6F_2) were used in the studies.

All mice were genotyped at the *Stat5b* locus by PCR as described below. As they were developed, congenic lines were also genotyped using microsatellite markers at or near 4 additional loci our lab has previously found to affect murine hepatocarcinogenesis: *D1Mit206* [32], *D4Mit31* and *D10Mit15* [33,34], and *D17Mit34* [35]. Additionally, the breakpoint on each side of the *Stat5b* locus was monitored during congenic development using microsatellite markers.

To generate *Tfm* animals (*Tfm*/Y), heterozygous *Tfm*/+ female and wild-type male mice were crossed and their offspring were genotyped as described below. Heterozygous *Tfm*/+ breeders were originally purchased from The Jackson Laboratories and backcrossed to C57BL/6J in our lab for more than 20 generations [12]. The *Tfm* mutation spontaneously arose in the B6 strain and is a frame-shift mutation in the androgen receptor gene [36]. To generate homozygous *little* animals (*Ghrhr*$^{lit/lit}$), heterozygous *Ghrhr*$^{lit/+}$ male mice were crossed with homozygous *Ghrhr*$^{lit/lit}$ females and genotyped as described below. B6-*lit/lit* mice were originally obtained from The Jackson Laboratories and maintained on a B6 background in our lab. The *little* mutation arose spontaneously in the B6 strain and is a point mutation in the *Ghrhr* gene [24].

All mice were treated in accordance with the NIH Guide for the Care and Use of Laboratory Animals. All experimental protocols were approved by the Animal Care and Use Committee of the School of Medicine and Public Health at the University of Wisconsin-Madison. Mice were housed in plastic cages on corncob bedding (Bed O'Cobs, Anderson Cob Division, Maumee, OH) and fed Mouse Diet 9F 5020 (9% fat; LabDiet, Madison, WI). All mice were given acidified tap water *ad libitum*. Animal health was monitored by daily inspection.

Genotyping

DNA was isolated from mouse tails or toes (at 9 to 14 days of age), and spleens (postmortem) using a standard proteinase-K-ammonium acetate precipitation protocol [32] or by alkaline lysis [37]. Briefly, DNA was isolated from tissues by alkaline lysis by incubation at 95 – 100°C in an alkaline solution (pH 12, 25 mM NaOH, 0.2 mM EDTA) for 20 to 40 minutes. The solution was neutralized by the addition of an acidic solution (pH 5, 40 mM Tris) and vortexed for 10 seconds. Tissue debris was removed by centrifugation at 16,000 *g*, and the supernatant was recovered and used for genotyping. The more rapid

alkaline lysis protocol was not compatible with the methods used for genotyping of *little* or *Tfm* mice.

All genotyping primers were purchased from Integrated DNA Technologies (Coralville, IA). Microsatellite markers were amplified using 1 to 2 μl of DNA (~100 ng) using standard conditions [32]. Genotyping of *little* and *Tfm* lines was performed by restriction digest of PCR products by *FokI* and *MwoI* respectively, as previously described [10,12]. Genotyping of *Stat5b*^{tm1Hwd} lines was performed using PCR as previously described [38]. All genotyping PCR products and digests were resolved by electrophoresis through a 7% polyacrylamide gel.

Liver Tumor Induction

The DEN-preweanling model was used for all hepatocarcinogenesis studies. Briefly, twelve-day-old mice (±1 day) were injected with *N*,*N*-diethylnitrosamine (DEN; Sigma, St. Louis, MO) intraperitoneally (i.p.) at a dose of 0.1 μmol/g body weight in tricaprylin (Sigma; 0.01 ml/g body weight) to initiate hepatocarcinogenesis. Males develop tumors earlier than females and were therefore aged to 32 weeks, while females were aged to 50 weeks before sacrifice [6–7,11–12]. At sacrifice, tumors >1 mm on the liver surface were enumerated and a tally of tumors >5 mm was also scored separately.

Gene Expression Analysis

At 10 weeks of age, DEN-initiated animals were sacrificed and a portion of their livers was stored in RNAlater (Ambion; Invitrogen, Calsbad, CA) for 4 days (±1 day) at 4°C, after which they were removed from RNAlater and stored long-term at −80°C. RNA was isolated from approximately 0.06 g whole liver using the RNeasy Midi Kit (Qiagen, Venlo, Netherlands) following the manufacturer's protocol, except 50% ethanol was substituted for 70% ethanol. RNA concentration was measured with a NanoDrop 1000 spectrophotometer (Thermo Fisher Scientific).

For microarray analysis, fluorescent Cy-3 probes were prepared independently from total RNA from three mice of each genotype using the Agilent Low Input Linear Amplification and Labeling Kit (Agilent Technologies, Santa Clara, CA). A reference, Cy-5 labeled probe was similarly prepared from a pool of C57BL/6 hepatic RNA constructed from equal quantities of male (15 individuals) and female (18 individuals) RNA. Before hybridization, probe concentrations were determined with a NanoDrop 1000 spectrophotometer (Thermo Fisher Scientific). Equal amounts of experimental and reference probe species (1.5 μg) were mixed and hybridized to the Whole Mouse Genome Microarray 4 x 44K (Agilent Technologies) according to the protocol provided by the manufacturer. The microarray slides were visualized using the Agilent Microarray Scanner System and analyzed with Agilent Feature Extraction Software v. 9.1. Gene expression was analyzed using EDGE v.3 [39] (developed by Drs. Christopher Bradfield and Aaron Vollrath, University of Wisconsin-Madison, Madison, WI) and Ingenuity Pathway Analysis (IPA) software (Ingenuity Systems, Redwood City, CA).

For measurement of specific mRNAs by quantitative real-time PCR (qPCR), cDNA was prepared from 5 μg of RNA by reverse transcription using the SuperScript II system (Invitrogen) following the manufacturer's specifications along with oligo(dT) 15 primer (Promega, Madison, WI) and 10 mM dNTPs (Roche). qPCR was performed on total cDNA diluted 1:16 using 500 nM of forward and reverse primers and 250 nM FAM-labeled probes with an internal ZEN™ quencher nine bases from the 5′ FAM and a 3′ Iowa Black™ quencher (PrimeTime™ qPCR assays, IDT). Primers and FAM-labeled probes were designed using IDT SciTools RealTime PCR design tool and primer locations were verified using BLAST (NCBI). A list of the primers and probes and their sequences and locations is given in Supplemental Table 1. Reactions were prepared in triplicate at 20 μl volumes in 384-well film-sealed plates (Applied Biosystems; Foster City, CA) and run on the ABI 7900HT (Applied Biosystems). For each reaction, AmpliTaq Gold PCR master mix (Applied Biosystems) was used at 1X and 0.4 uL of ROX reference dye was added (Invitrogen, Carlsbad, CA). The thermocycling protocol was one cycle of 50°C for 2 minutes and 95°C for 10 minutes, followed by 40 cycles of 95°C for 15 seconds and 60°C for 1 minute. Controls with no cDNA template or no reverse transcriptase were conducted for each group. A standard curve (1:2 to 1:64) was performed to verify that the amplification efficiency of the housekeeping gene, *Actb*, was suitable for delta-delta-Ct analysis [40]. Fold-change values were calculated using the delta-delta-Ct method [40] using *Actb* as a housekeeping gene and normalizing the expression relative to the wild-type male of the appropriate genetic background.

Immunoblot analysis

The primary rabbit antibodies anti-pY-STAT3 (Tyr705; CS#9145), anti-pY-STAT5 (Tyr694; CS#4322), anti-Stat3 (CS#4904), anti-Stat5 (CS#9363), anti-β-actin (CS#4970) and HRP-linked goat anti-rabbit (CS#7074) secondary antibody were purchased from Cell Signaling (Beverly, MA). Protein was extracted from snap-frozen whole liver harvested from 10- to 12-week-old mice in a liquid nitrogen-cooled mortar. Tissue was ground into a fine powder and suspended in RIPA buffer (Thermo Fisher Scientific) with 2X Halt Protease and Phosphatase Inhibitor Cocktail (Thermo Fisher Scientific). Total protein concentration was determined by BCA assay (Thermo Fisher Scientific); 40 μg of protein was loaded and separated on pre-cast 4–20% polyacrylamide gels (Thermo Fisher Scientific) and electrotransferred to a PVDF membrane (Millipore, Billerica, MA). Blots were blocked with 5% low fat milk at RT for 1 hour, then incubated with primary antibodies at 1:1000 (except for anti-STAT3 which was used at 1:2000) dilution in 5% BSA in 1X TBS, 0.1% Tween-20 (TBS-T) overnight at 4°C or at RT for 1–2 hours. Membranes were washed 2 times for 15 minutes in 1X TBS-T. Membranes were then incubated with HRP-linked goat anti-rabbit IgG (Cell Signaling) secondary antibody diluted at 1:3000 in 5% BSA for 1 hour at RT. Membranes were washed again as described above. All blots were visualized using ECL PLUS (GE Healthcare; Little Chalfont, UK) following the manufacturer's protocol. A film image was acquired using diagnostic film (Eastman Kodak) and the fluorescent product was visualized by scanning on a Storm 840 Imager (GE Healthcare) in fluorescence acquisition mode with excitations at 635 and 450 nm, normal sensitivity, PMT 800V, and a pixel size of 200 μm.

Histology and Immunohistochemistry

Liver tumors were fixed in 10% neutral buffered formalin (NBF) at 4°C for 2 to 6 days. The samples were then transferred to 70% ethanol for long-term storage at 4°C until paraffin embedding. Pituitaries were removed from 10-week-old animals at sacrifice. Briefly, the whole head was removed with heavy scissors. A lateral cut in the skin was made along the center of the skull from the back of the head to between the eyes. This skin was pulled back on both sides, and the exposed skull was cut in a similar manner. A cut above each eye was made and the skull was peeled back to expose the brain. The brain was carefully removed, exposing the pituitary. The part of the skull containing the pituitary was carefully removed, with pituitary, and immediately placed in NBF and stored overnight at 4°C. The following day, the pituitary was gently separated from the skull and associated connective tissue with the assistance of a dissection microscope. The pituitary was then weighed and transferred to a 70% ethanol solution and stored at 4°C. Multiple pituitaries were embedded in a 2% agar: 2.5% gelatin mixture as previously described, then stored in 70% ethanol at 4°C prior to paraffin embedding [41]. Pituitary specimens were isolated, fixed and prepared as described as above.

Embedding and subsequent sectioning and staining was performed by the UWCCC Experimental Pathology Core Service. Briefly, tissues were removed from 70% ethanol, dehydrated, paraffin infiltrated, and paraffin embedded. Sections were cut at 5 μm and mounted on slides for all downstream staining procedures. H&E staining was performed for liver tumor histopathology and pituitary analysis.

IHC for pY-STAT3 (Tyr705; CS#9145) and pY-STAT5 (Tyr694; CS#9359) was performed using primary antibodies from Cell Signaling (Beverly, MA) following the manufacturer's instructions, using pH 8 EDTA for antigen retrieval and a 1:400 dilution for both primary antibodies. IHC for GH and prolactin was performed using anti-GH and –prolactin antibodies from Dr. Albert Parlow (The National Hormone & Peptide Program, UCLA) at a 1:3200 dilution. Briefly, slides were deparaffinized in xylene and hydrated through graded ethyl alcohols to water. Slides were washed with phosphate buffered saline (PBS) three times. Non-specific binding was blocked with 10% goat serum in PBS for one hour and endogenous peroxidase was blocked with 0.3% hydrogen peroxide in PBS for 10 minutes. Endogenous biotin was blocked with 0.001% avidin in PBS for ten minutes and the avidin quenched with 0.001% biotin in PBS for ten minutes. The slides were then incubated with primary antibody diluted in PBS with 1% goat serum overnight at 4°C. After washing with PBS three times, the sections were incubated with biotinylated goat anti-rabbit (Vector Laboratories, Burlingame, CA) at 1:200 in PBS for one hour at room temperature. Slides were washed in PBS three times, then incubated 30 minutes at room temperature with Vectastain ABC Elite (Vector Laboratories). Following three washes in PBS, slides were developed with DAB (Vector Laboratories), counterstained with Mayer's hematoxylin, dehydrated and cover slipped with permount. All reagents and chemicals are from Sigma (St. Louis, MO) unless otherwise noted.

Statistical analysis

For microarray analysis of gene expression, adjusted p-values were generated on EDGE v.3 using the Linear Models for Microarray Data (LIMMA) software package with the Benjamini-Hochberg false discovery rate (FDR) correction [42]. The Spearman rank correlation test was used to compare genotypes for the fold-changes of differentially expressed genes. Pathway analysis was performed using the IPA software package and Fisher's exact test was used to determine significant differences between groups in the representation of gene sets. The Wilcoxon Rank Sum test [43] was used to determine the significance of differences in tumor multiplicity and pituitary weight as a function of *Stat5b* genotype; *P*-values were corrected for multiple comparisons within each strain/sex combination by the Dunn-Šidák method [44]. The *Mstat* software package (Dr. Norman Drinkwater, University of Wisconsin-Madison, WI, http://www.mcardle.wisc.edu/mstat/) was used for these statistical tests.

Results

Most androgen- and STAT5b-sensitive hepatic genes are also growth hormone-sensitive

To assess gene expression in the *Tfm*, *little*, and *Stat5b* inbred strains, we hybridized liver RNA from 10-week-old, DEN-treated mice to Agilent whole-genome microarrays. We found a high degree of overlap among differentially expressed (DE) genes in the livers of *Tfm*, *little*, and *Stat5b*-deficient mice, and the degree of differential expression relative to wild-type was highly correlated among the mutants. Spearman rank correlation coefficients ranged from 0.64, for *Tfm* versus B6 STAT5b KO, to 0.8, for *little* versus *Tfm*, with *P*-values less than 10^{-57} (Table 1, Figure 1). This striking overlap is also illustrated in a heatmap of the combined set of all highly significant DE genes for each mutant (Supp. Figure 1). Generally, genes that were DE in *Tfm* and/or STAT5b KO males were also DE in *little* males. A list of the 25 most significantly DE genes for C57BL/6J and BALB/c STAT5b KO, *little*, and *Tfm* males further illustrates their overlap (Supp. Table 2).

We used IPA software to identify the molecular and cellular functions enriched in DE genes from each experimental group. We found similar categories enriched in DE genes in *Tfm*, *little*, and STAT5b KOs, such as lipid metabolism, energy production, and small molecule biochemistry. The top category for both STAT5b KO congenics was cell morphology. Additionally, DE genes from both STAT5b KO congenics were enriched in the category of antigen presentation. We also used IPA to identify transcription factors and transcription factor complexes whose targets are enriched in DE genes for each experimental group (Table 2). The DE genes in *Tfm*, *little*, and STAT5b KO males are most highly enriched with targets of transcription factors *Rora* and *Rorc*, although the mRNA levels of these two transcription factors are not altered.

To validate our microarray results, we performed qPCR for a set of DE genes and sex-specific genes that had previously been shown to be regulated by growth hormone [20–23]. The microarray values were very similar to the qPCR values for most of the genes examined (Supp. Table 3). Spearman's rank correlation test was used to determine if there was significant correlation between the fold-change values measured by qPCR and by

microarray. For each group (*Tfm*, *little*, B6 STAT5b KO, and BALB STAT5b KO), the qPCR values were significantly correlated with the microarray values ($P = 0.001$, 0.0006, 0.0003, and 0.0002 respectively).

Genetic background determines whether STAT5b knockout suppresses or enhances murine hepatocarcinogenesis

The tumor susceptibility of global STAT5b KOs varied depending on the genetic background. For both males and females, STAT5b KO did not affect tumor multiplicity on the BALB/cJ background. At 32 weeks of age, wild-type and knockout C.129-$N_{11}F_2$*Stat5b*^{tm1Hwd} males averaged 7.6 and 10 tumors per animal, respectively, with no significant difference ($P = 0.99$; Table 3). Heterozygous males developed fewer tumors than either wild-type ($P = 0.025$) or null ($P = 0.07$) mice, perhaps due to overdominance. At 50 weeks of age, wild-type and knockout C.129-$N_{11}F_2$*Stat5b*^{tm1Hwd} females averaged 12 and 11 tumors per animal, respectively, with no significant difference ($P = 0.98$).

In contrast, both male and female B6 STAT5b KOs were more sensitive to hepatocarcinogenesis than their wild-type littermates. At 32 weeks of age, B6 STAT5b knockout male congenics had 2.4-fold more tumors per animal than wild-type males, with mean tumor multiplicities of 52 and 22, respectively ($P = 0.002$). By 50 weeks, STAT5b knockout females also developed 2.4-fold more tumors per animal than their wild-type female littermates (40 versus 17 tumors per mouse; $P = 0.0003$). The B6 STAT5b-congenic mice also developed more large liver tumors (> 5 mm in diameter). For males, the mean number of large tumors increased from 0.6 for wild-type to 3.2 for homozygous mutant mice ($P = 0.003$), while females developed 0.6 and 2.6, respectively (P = 0.002). The susceptibility conferred by STAT5b loss was recessive.

In both sexes, STAT5b KOs on the C3H background (C3.129-N_6F_2*Stat5b*^{tm1Hwd} congenics) had significantly fewer tumors per animal than their wild-type littermates. At 32 weeks, STAT5b knockout males had 2.7-fold fewer tumors than their wild-type littermates (mean tumor multiplicities 51 and 136; $P = 0.02$). By 50 weeks, C3H STAT5b knockout females had almost 6-fold fewer tumors than their wild-type littermates. Wild-type females averaged 59 tumors per animal, while STAT5b knockout females averaged 10 tumors per animal ($P = 0.01$). As for B6 congenics, the effect of STAT5b loss in C3H congenics was recessive.

Although we found differences in tumor susceptibility among STAT5b KO congenics, their tumors were histologically similar. In both wild-type and STAT5b KO mice of each strain, approximately equal numbers of Type A hepatic adenomas and Type B (or mixed Type A and B) hepatocellular carcinomas were observed.

STAT3 and STAT5 activation in STAT5b knockout livers

To determine whether the susceptibility of B6 STAT5b KO mice relative to BALB STAT5b KO mice correlates with STAT5 protein levels, total STAT5 (STAT5a and STATb) and phospho-STAT5 (Y694) were measured by Western blot in livers isolated from 10-week-old male and female mice (Figures 2A and 2B). For both B6 and BALB congenics, STAT5b KO

males and females had reduced levels of total STAT5 protein. High levels of pY-STAT5 were limited to WT males.

In addition to STAT5b, growth hormone can activate STAT3. Previous reports have implicated aberrant GH-induced activation of STAT3 in the absence of STAT5 with increased liver cancer development [45,46]. We found similar levels of STAT3 and pY-STAT3 between WT and KO animals for both B6 and BALB congenics, as detected by Western blot (data not shown). Detection of pY-STAT3 in tumor sections was generally isolated to a few clusters of positive cells. Though limited, pY-STAT3 was detected in both wild-type and STAT5b KO tumors from both sexes and from both B6 and BALB congenics (data not shown).

Strain-dependent effect of STAT5b knockout on pituitary size

It has been reported that global and *Stat5*$^{\Delta hep}$ liver-specific STAT5b knockout mice have elevated GH levels [31,47]. We wondered if the differences in susceptibility we found among STAT5b KO strains were due to differences in elevated GH in response to STAT5b loss. Due to the pulsatile nature of GH release profile, it is difficult to assess GH levels directly in mice. Pituitary size has been shown to correlate with levels of GH [48,49]; therefore, we assessed GH differences among B6 STAT5b KO, BALB STAT5b KO, and corresponding wild-type strains using the pituitary as a surrogate. Formalin-fixed pituitaries from 10-week-old mice were isolated and weighed. For both sexes, B6 STAT5b KO mice had 1.5-fold larger pituitaries than their WT littermates (Figure 3). The average mass of pituitaries from C57BL/6J STAT5b KO males was 2.9 ± 0.3 mg, whereas pituitaries from their wild-type littermates had a mass of 2.0 ± 0.2 mg ($P = 2\times10^{-6}$). Pituitaries from B6 STAT5b KO and WT females weighed 3.8 ± 0.4 mg and 2.4 ± 0.3 mg, respectively ($P = 4\times10^{-7}$). Histological analysis of these pituitaries revealed that the enlarged region of the B6 KO pituitaries was the pars distalis, which secretes hormones (Supp. Figure 2). Immunohistochemistry revealed that the distribution of GH- and prolactin-secreting cells was not altered between WT and KO pituitaries, but due to the increased size of the pars distalis in KO pituitaries, there are more of these cells (data not shown).

Pituitaries from 10-week-old BALB STAT5b KO mice were isolated and weighed as above. In contrast to B6 STAT5b KO males, pituitaries from BALB STAT5b KO males were not significantly larger than their wild-type littermates (Figure 4). The average mass of pituitaries from both BALB STAT5b KO males and their wild-type littermates was 2.0 mg ($P = 0.70$). However, BALB STAT5b KO females (3.2 ± 0.3 mg) did have significantly larger pituitaries than their wild-type littermates (2.5 ± 0.4 mg) ($P = 0.0004$).

DISCUSSION

Our initial hypothesis was that STAT5b is required for male-specific sensitivity to hepatocarcinogenesis. We formed this hypothesis based on several findings from the past few decades. Hepatocarcinogenesis studies in gonadectomized mice demonstrated the opposing effects of sex hormones on liver cancer development [50]. Research with *Tfm* mice showed that testosterone-mediated promotion of liver cancer requires functional androgen receptor and is not cell autonomous [10]. GH-deficient *little* mice revealed that wild-type

levels of GH are required for susceptibility to liver cancer [12]. Downstream from GH, the transcription factor STAT5b is thought to be the master regulator of sex-specific hepatic gene expression in response to the pulsatile plasma GH profile characteristic of males [51]. Of genes exhibiting male bias, 90% were down-regulated in global STAT5b knockout males [29]. Thus, STAT5b is thought to be required for male hepatic gene expression.

Our microarray results were largely supportive of our hypothesis, that testosterone-activated AR, GH, and STAT5b all work in a shared pathway to affect hepatic gene expression in males. Pairwise correlations for the regulation of differentially expressed genes in the *little*, *Tfm*, and the B6 and BALB/c STAT5b KO strains were all highly significant (*P*-values between 10^{-57} and 10^{-121}). Pathway analysis revealed several shared categories of molecular and cellular functions enriched in DE genes among *Tfm*, *little*, and STAT5b KOs. These pathways include lipid metabolism, small molecule biochemistry, energy production, and molecular transport (data not shown). The genes affecting lipid metabolism include sex-specific CYPs involved in steroid metabolism, members of the ABC ATP-binding cassette family, acyl-CoA thioesterases and synthetases, growth factors and their receptors, hydroxysteroid 11-beta dehydrogenases, peroxisome proliferator activated receptor gamma members, solute carrier transporter family members, and serine (or cysteine) peptidase inhibitors. Together, these genes affect lipid and cholesterol levels by affecting their synthesis, metabolism, storage and transport. Lipid metabolism is emerging as a factor increasingly relevant to human HCC [4,52]. Steroid metabolism affects the bioavailability of sex hormones, which we and others have shown affect murine hepatocarcinogenesis. In addition, energy metabolism changes are hallmarks of cancer, as cancer cells must be supplied with the necessary fuel and nutrients to support their rapid division and expansion [53].

Pathway analysis also found common transcriptional programs enriched among DE genes of *Tfm*, *little*, and STAT5b KOs (Table 2). As expected, targets of STAT5b were differentially expressed in these strains, reflecting decreased STAT5b activity in resistant mutants and STAT5b KOs. However, targets of other transcription factors were more significantly differentially regulated than those of STAT5b. Among DE genes in *Tfm*, *little*, and STAT5b KOs, the most significantly affected sets of transcription factor targets were those of Rora and Rorc. The overlap between DE genes and Rora and Rorc targets was strikingly significant. For example, for *little* males the significance of the overlap for Rorc and Rora was $P = 4.7\times10^{-22}$ and $P = 1.9\times10^{-21}$, whereas the next most significant overlap was with *Nr1i3* ($P = 3.8\times10^{-11}$), and the significance of the overlap for *Stat5b* was 8.0×10^{-6}.

We were surprised Stat5b was not the transcription factor with the most significant overlap, which might indicate imperfect pathway prediction. Alternatively, the lower ranking of Stat5b might reflect the fact that transcription factors downstream of Stat5b (such as Rorc and Rora) have manifold effects on gene expression that differ among strains because these transcription factors are polymorphic or are differentially activated. Consistent with this alternative explanation, Rora activity was predicted to be activated in *little* and BALB KOs but inhibited in B6 KOs. Differences in susceptibility between B6 and BALB KOs might be due to differences in Rora activation. Rora might therefore be a better candidate than *Stat5b* for the mediator of male-specific sensitivity to liver cancer.

Although a vast majority of gene expression changes were concordant among the mutants (Figure 1), there were exceptions. For example, *Ptk2b*, a regulatory tyrosine kinase, was the 7th most significant DE gene ($P = 1.2 \times 10^{-10}$) for B6 STAT5b KOs (FC = −3.4) but was not significantly DE for BALB STAT5b KOs (P = 0.73, FC = −0.3) (Supp. Table 2). Additionally, *Spink6*, a serine protease inhibitor selective for kallikreins, was the14th most significant DE gene ($P = 2.0 \times 10^{-9}$) for BALB STAT5b KOs (FC = −5.3) but was not significantly DE for B6 STAT5b KOs (P = 1, FC = 0). Discordant DE genes between B6 and BALB STAT5b KOs are potentially responsible for their differences in liver cancer susceptibility.

We examined the effect of STAT5b KOs on DEN-induced hepatocarcinogenesis on three distinct genetic backgrounds (Table 3). Each background yielded a distinct tumor susceptibility phenotype. We saw no difference in the average tumor multiplicities of BALB/cJ STAT5b KO mice in comparison to wild-type controls. On the more sensitive C57BL/6J background, we observed higher average tumor multiplicities in STAT5b KOs from either sex than in wild-type controls. Both male and female STAT5b KOs averaged 2.4-fold more tumors than B6 controls. Further, STAT5b KOs from both sexes had more large tumors, averaging 5-fold more than controls.

The effect of STAT5b KO on the third genetic background, C3H/HeJ, was as predicted by our original hypothesis: STAT5b was required for susceptibility. Both male and female STAT5b KOs of the C3H/HeJ background averaged fewer tumors than wild-type controls (Table 3). Male STAT5b KOs averaged 2.7-fold fewer tumors than controls, and female STAT5b KOs averaged about 6-fold fewer tumors than controls. Unfortunately, due to poor breeding in this line, the sample size was much lower for our C3H/HeJ study than for the BALB/cJ and C57BL/6J studies. Additionally, the entire C3H/HeJ STAT5b KO production went into the tumor study, so we were unable to perform gene expression analysis on C3H/HeJ congenics. Nonetheless, the decrease in tumor multiplicity was significant for both males and females, with $P < 0.02$ for both.

The most likely explanation for the different phenotypes of the inbred *Stat5b* congenics is that the B6, BALB, and C3H inbred strains carry different modifiers of the STAT5b pathway. An initial analysis of unlinked loci previously identified as affecting strain-specific susceptibility to hepatocarcinogenesis (*D1Mit206* [32], *D4Mit31* and *D10Mit15* [33,34], and *D17Mit34* [35]) indicated that these loci were not responsible for differences in susceptibility in STAT5b KOs (data not shown).

An alternative explanation for the congenic strains' different STAT5b KO phenotypes is that modifiers lie in the congenic region that was introgressed into the B6 and C3H genetic backgrounds, and that different congenic strains may have inherited congenic regions that carry different sets of modifiers. The donor strain for the creation of the B6 and C3H congenics was the C.129-N_5F_2Stat5b^{tm1Hwd} line; therefore, the linked modifiers would consist of BALB or 129 loci. The maximal 129-derived region surrounding the linked *Stat5b* locus on Chromosome 11 in each of our congenic lines in the BALB line was about 22 Mb (containing roughly 725 genes), as the breeders were homozygous BALB at 80 Mb and 102.5 Mb on Chromosome 11 (*Stat5b* is located at ~100 Mb). We identified some

heterogeneity among the endpoints of the congenic region in the B6 and C3H strains, at up to 10 and 20 Mb proximal (350 to 595 genes) and up to 9 and 13 Mb distal (320 to 415 genes) of the *Stat5b* gene, respectively (data not shown).

Hypophysectomy experiments have provided evidence of the pro-oncogenic properties of pituitary hormones, which are partially attributed to GH [54–57]. We found that male and female B6 STAT5b KOs had significantly larger pituitaries than wild-type mice, whereas, among BALB STAT5b KO mice, only females had significantly larger pituitaries (Figure 3). This increase in pituitary size was limited to the pars distalis, the hormone-secreting portion of the pituitary. Pituitary alterations in B6 KO mice might lead to increased levels of circulating pituitary hormones that promote liver cancer, such as GH and prolactin, or modulate sex hormone levels via FSH or LH. It has been reported that global STAT5b and $STAT5^{\Delta hep}$ knockout mice have elevated circulating GH levels, and perhaps this is due, in part, to an expanded pars distalis [31,47]. However, an expanded pars distalis does not necessarily correlate with susceptibility: BALB STAT5b KO females, which also had larger pituitaries, were not more sensitive to liver cancer development.

Recently, two other murine liver cancer studies involving STAT5 have shown increased hepatocarcinogenesis in STAT5b KOs, similar to our findings with C57BL/6J congenics. The first study examined the role of STAT5 in murine carcinogenesis in $STAT5^{\Delta hep}$ mice [45]. These animals were treated with carbon tetrachloride (CCl_4). After 8 weeks of CCl_4 treatment, 20% (4 out of 20) of $STAT5^{\Delta hep}$ mice developed HCC, whereas none were detected in the 26 control mice ($P = 0.02$). The loss of STAT5 regulation of TGF-β and increased GH-mediated activation of STAT3 were the mechanisms the authors suggested might explain the increased sensitivity to hepatocarcinogenesis in $STAT5^{\Delta hep}$ mice. The floxed *Stat5* animals were a mix of FVB/N and NIH Black Swiss backgrounds [58]. The albumin-cre transgenics were on the FVB/N background.

The second recent STAT5-related carcinogenesis study examined hepatocarcinogenesis in $STAT5^{\Delta hep}$ mice in the context of GH over-expression [46]. These $GH^{tg}STAT5^{\Delta hep}$ mice displayed earlier and more advanced spontaneous HCC than GH^{tg} mice. However, $GH^{tg}STAT5^{\Delta hep}$ mice did not display many of the phenotypes presented in GH^{tg} mice, such as gigantism, premature mortality, chronic hepatic inflammation, and many of the pathologic hepatocyte alterations. $STAT5^{\Delta hep}$ mice, in the absence of transgenic GH, did not develop spontaneous HCC. The authors attribute the enhanced HCC in $GH^{tg}STAT5^{\Delta hep}$ mice to increased peripheral lipolysis, increased hepatic lipid synthesis, accumulation of DNA damage as a result of disturbed cell-cycle control, and aberrant activation of c-JUN and STAT3. The genetic background of the $GH^{tg}STAT5^{\Delta hep}$ mice was, as with $STAT5^{\Delta hep}$ mice, mixed FVB/N and NIH Black Swiss and less defined than the STAT5b knockout congenics lines we used.

In conclusion, we found that STAT5b is likely not the sole molecular mediator of male-specific sensitivity to hepatocarcinogenesis in mice. Further, we found that genetic background determines whether STAT5b KO enhances or suppresses murine hepatocarcinogenesis. The ability of *Stat5b* to act as both tumor suppressor and oncogene in the liver was surprising. These opposite effects are likely to be caused by the interaction of

STAT5b with strain-specific modifiers of hepatocarcinogenesis. Previous studies have shown that an EGF receptor disruption can cause dramatically different phenotypes in different inbred strains [59]. Other studies have shown that expression levels and genetic background determine whether the cyclin-dependent-kinase-associated protein p21 suppresses or promotes tumorigenesis, depending on the tissue in which the gene acts [60]. Yet others have shown that the *Mus spretus* allele of Kras2 can confer resistance or susceptibility in the lung, depending on the allele of its homologous pair [61]. This analysis of *Stat5b* is the first study, to our knowledge, to show that a single mutation can have opposite effects on carcinogenesis in a single tissue, depending only on the endogenous alleles in the genetic backgrounds of inbred strains.

The observation that genes unrelated to a cancer modifier can affect the phenotype of that modifier qualitatively has implications for human liver cancer, as human populations exhibit a high degree of genetic heterogeneity. Further characterization of the genetic elements responsible for the range of effect we observed among BALB/cJ, C57BL/6J, and C3H/HeJ mice could have translational benefit, potentially helping to identify patients who would benefit from therapies targeted to the GH pathway.

Supplementary Material

Refer to Web version on PubMed Central for supplementary material.

Acknowledgments

Grant Support: This work was supported by grants CA009135, CA14520, CA96654, and CA22484 from the National Cancer Institute of the National Institutes of Health.

The authors wish to thank Ms. Rebecca Baus and the staff of the McArdle Animal Care Facility for their help with the mice, Dr. Henry Pitot for his expertise in histopathology, Dr. Chris Bradfield for his advice on the microarray analyses, and the Experimental Pathology Shared Service of the UW Carbone Comprehensive Cancer Center for their help with the immunohistochemistry.

Abbreviations

GH	growth hormone
STAT5b	signal transducer and activator of transcription 5b
STAT5b KO	STAT5b knockout
BALB	BALB/cJ
B6	C57BL/6J
C3H	C3H/HeJ
WT	wild-type
HCC	hepatocellular carcinoma
Tfm	testicular feminization
CYPs	cytochrome P450 enzymes

Ghrhr	growth-hormone-releasing-hormone receptor
IPA	Ingenuity Pathway Analysis
LIMMA	Linear Models for Microarray Data
FDR	false discovery rate
qPCR	quantitative real-time PCR
DEN	*N*,*N*-diethylnitrosamine
NBF	neutral buffered formalin
IHC	immunohistochemistry
PBS	phosphate-buffered saline
DE	differentially expressed

References

1. Ferlay J, Shin H-R, Bray F, Forman D, Mathers C, Parkin DM. Estimates of worldwide burden of cancer in 2008: GLOBOCAN 2008. Int J Cancer. 2010; 127:2893–2917. [PubMed: 21351269]
2. Altekruse SF, McGlynn KA, Reichman ME. Hepatocellular carcinoma incidence, mortality, and survival trends in the United States from 1975 to 2005. J Clin Oncol. 2009; 27:1485–1491. [PubMed: 19224838]
3. El-Serag HB, Mason AC. Rising incidence of hepatocellular carcinoma in the United States. N Engl J Med. 1999; 340:745–750. [PubMed: 10072408]
4. El-Serag HB, Rudolph KL. Hepatocellular carcinoma: epidemiology and molecular carcinogenesis. Gastroenterology. 2007; 132:2557–2576. [PubMed: 17570226]
5. Smith GS, Walford RL, Mickey MR. Lifespan and incidence of cancer and other diseases in selected long-lived inbred mice and their F1 hybrids. J Natl Cancer Inst. 1973; 50:1195–1213. [PubMed: 4351393]
6. Vesselinovitch SD, Mihailovich N. The effect of gonadectomy on the development of hepatomas induced by urethan. Cancer Res. 1967; 27:1788–1791. [PubMed: 4294315]
7. Kemp CJ, Drinkwater NR. Genetic variation in liver tumor susceptibility, plasma testosterone levels, and androgen receptor binding in six inbred strains of mice. Cancer Res. 1989; 49:5044–5047. [PubMed: 2766275]
8. Toh YC. Effect of neonatal castration on liver tumor induction by N-2-fluorenylacetamide in suckling BALB/c mice. Carcinogenesis. 1981; 2:1219–1221. [PubMed: 7318159]
9. Andervont HB. Studies on the occurrence of spontaneous hepatomas in mice of strains C3H and CBA. J Natl Cancer Inst. 1950; 11:581–592. [PubMed: 14824917]
10. Kemp CJ, Leary CN, Drinkwater NR. Promotion of murine hepatocarcinogenesis by testosterone is androgen receptor-dependent but not cell autonomous. Proc Natl Acad Sci USA. 1989; 86:7505–7509. [PubMed: 2798421]
11. Poole TM, Drinkwater NR. Strain dependent effects of sex hormones on hepatocarcinogenesis in mice. Carcinogenesis. 1996; 17:191–196. [PubMed: 8625437]
12. Bugni JM, Poole TM, Drinkwater NR. The *little* mutation suppresses DEN-induced hepatocarcinogenesis in mice and abrogates genetic and hormonal modulation of susceptibility. Carcinogenesis. 2001; 22:1853–1862. [PubMed: 11698349]
13. Yamamoto R, Iishi H, Tatsuta M, Tsuji M, Terada N. Roles of ovaries and testes in hepatocellular tumorigenesis induced in mice by 3′-methyl-4-dimethylaminoazobenzene. Int J Cancer. 1991; 49:83–88. [PubMed: 1874575]

14. Naugler WE, Sakurai T, Kim S, et al. Gender disparity in liver cancer due to sex differences in MyD88-dependent IL-6 production. Science. 2007; 317:121–124. [PubMed: 17615358]
15. Li Z, Tuteja G, Schug J, Kaestner KH. Foxa1 and Foxa2 are essential for sexual dimorphism in liver cancer. Cell. 2012; 148:72–83. [PubMed: 22265403]
16. Jansson JO, Edén S, Isaksson O. Sexual dimorphism in the control of growth hormone secretion. Endocr Rev. 1985; 6:128–150. [PubMed: 2861084]
17. Jansson JO, Ekberg S, Isaksson OG, Edén S. Influence of gonadal steroids on age- and sex-related secretory patterns of growth hormone in the rat. Endocrinology. 1984; 114:1287–1294. [PubMed: 6705738]
18. MacLeod JN, Pampori NA, Shapiro BH. Sex differences in the ultradian pattern of plasma growth hormone concentrations in mice. J Endocrinol. 1991; 131:395–399. [PubMed: 1783886]
19. Veldhuis JD, Bowers CY. Human GH pulsatility: an ensemble property regulated by age and gender. J Endocrinol Invest. 2003; 26:799–813. [PubMed: 14964431]
20. Waxman DJ, Pampori NA, Ram PA, Agrawal AK, Shapiro BH. Interpulse interval in circulating growth hormone patterns regulates sexually dimorphic expression of hepatic cytochrome P450. Proc Natl Acad Sci USA. 1991; 88:6868–6872. [PubMed: 1862110]
21. Zhang Y, Klein K, Sugathan A, et al. Transcriptional profiling of human liver identifies sex-biased genes associated with polygenic dyslipidemia and coronary artery disease. PLoS ONE. 2011; 6:e23506. [PubMed: 21858147]
22. Wauthier V, Waxman DJ. Sex-specific early growth hormone response genes in rat liver. Mol Endocrinol. 2008; 22:1962–1974. [PubMed: 18483176]
23. Wauthier V, Sugathan A, Meyer RD, Dombkowski AA, Waxman DJ. Intrinsic sex differences in the early growth hormone responsiveness of sex-specific genes in mouse liver. Mol Endocrinol. 2010; 24:667–678. [PubMed: 20150183]
24. Eicher EM, Beamer WG. Inherited ateliotic dwarfism in mice. Characteristics of the mutation, little, on chromosome 6. J Hered. 1976; 67:87–91. [PubMed: 1270792]
25. Godfrey P, Rahal JO, Beamer WG, Copeland NG, Jenkins NA, Mayo KE. GHRH receptor of *little* mice contains a missense mutation in the extracellular domain that disrupts receptor function. Nat Genet. 1993; 4:227–232. [PubMed: 8395283]
26. Lin SC, Lin CR, Gukovsky I, Lusis AJ, Sawchenko PE, Rosenfeld MG. Molecular basis of the *little* mouse phenotype and implications for cell type-specific growth. Nature. 1993; 364:208–213. [PubMed: 8391647]
27. Waxman DJ, Ram PA, Park SH, Choi HK. Intermittent plasma growth hormone triggers tyrosine phosphorylation and nuclear translocation of a liver-expressed, Stat 5-related DNA binding protein. Proposed role as an intracellular regulator of male-specific liver gene transcription. J Biol Chem. 1995; 270:13262–13270. [PubMed: 7768925]
28. Choi HK, Waxman DJ. Growth hormone, but not prolactin, maintains low-level activation of STAT5a and STAT5b in female rat liver. Endocrinology. 1999; 140:5126–5135. [PubMed: 10537141]
29. Clodfelter KH, Holloway MG, Hodor P, Park S-H, Ray WJ, Waxman DJ. Sex-dependent liver gene expression is extensive and largely dependent upon signal transducer and activator of transcription 5b (STAT5b): STAT5b-dependent activation of male genes and repression of female genes revealed by microarray analysis. Mol Endocrinol. 2006; 20:1333–1351. [PubMed: 16469768]
30. Teglund S, McKay C, Schuetz E, et al. Stat5a and Stat5b proteins have essential and nonessential, or redundant, roles in cytokine responses. Cell. 1998; 93:841–850. [PubMed: 9630227]
31. Udy GB, Towers RP, Snell RG, et al. Requirement of STAT5b for sexual dimorphism of body growth rates and liver gene expression. Proc Natl Acad Sci USA. 1997; 94:7239–7244. [PubMed: 9207075]
32. Bilger A, Bennett LM, Carabeo RA, et al. A potent modifier of liver cancer risk on distal mouse chromosome 1: linkage analysis and characterization of congenic lines. Genetics. 2004; 167:859–866. [PubMed: 15238534]
33. Lee GH, Bennett LM, Carabeo RA, Drinkwater NR. Identification of hepatocarcinogen-resistance genes in DBA/2 mice. Genetics. 1995; 139:387–395. [PubMed: 7705639]

34. Lee GH, Ogawa K, Nishimori H, Drinkwater NR. Most liver epithelial cell lines from C3B6F1 mice exhibit parentally-biased loss of heterozygosity at the Lci (Liver cell immortalization) locus on chromosome 4. Oncogene. 1995; 11:2281–2287. [PubMed: 8570178]
35. Peychal SE, Bilger A, Pitot HC, Drinkwater NR. Predominant modifier of extreme liver cancer susceptibility in C57BR/cdJ female mice localized to 6 Mb on chromosome 17. Carcinogenesis. 2009; 30:879–885. [PubMed: 19255062]
36. He WW, Kumar MV, Tindall DJ. A frame-shift mutation in the androgen receptor gene causes complete androgen insensitivity in the testicular-feminized mouse. Nucleic Acids Res. 1991; 19:2373–2378. [PubMed: 2041777]
37. Truett GE, Heeger P, Mynatt RL, Truett AA, Walker JA, Warman ML. Preparation of PCR-quality mouse genomic DNA with hot sodium hydroxide and tris (HotSHOT). Biotechniques. 2000; 29:52–54. [PubMed: 10907076]
38. Grattan DR, Xu J, McLachlan MJ, et al. Feedback regulation of PRL secretion is mediated by the transcription factor, signal transducer, and activator of transcription 5b. Endocrinology. 2001; 142:3935–3940. [PubMed: 11517172]
39. Vollrath AL, Smith AA, Craven M, Bradfield CA. EDGE3: A web-based solution for management and analysis of Agilent two color microarray experiments. BMC Bioinformatics. 2009; 10:280. [PubMed: 19732451]
40. Pfaffl MW. A new mathematical model for relative quantification in real-time RT-PCR. Nucleic Acids Res. 2001; 29:e45. [PubMed: 11328886]
41. Jones MV, Calabresi PA. Agar-gelatin for embedding tissues prior to paraffin processing. BioTechniques. 2007; 42:569–570. [PubMed: 17515193]
42. Smyth GK. Linear models and empirical bayes methods for assessing differential expression in microarray experiments. Stat Appl Genet Mol Biol. 2004; 3:Article3. [PubMed: 16646809]
43. Hollander, M.; Wolfe, DA.; Chicken, E. Nonparametric statistical methods. Hoboken: Wiley; 2013. p. 819
44. Ury HK. A comparison of four procedures for multiple comparisons among means (pairwise contrasts) for arbitrary sample sizes. Technometrics. 1976; 18:89–97.
45. Hosui A, Kimura A, Yamaji D, Zhu B, Na R, Hennighausen L. Loss of STAT5 causes liver fibrosis and cancer development through increased TGF-β and STAT3 activation. J Exp Med. 2009; 206:819–831. [PubMed: 19332876]
46. Friedbichler K, Themanns M, Mueller KM, et al. Growth-hormone-induced signal transducer and activator of transcription 5 signaling causes gigantism, inflammation, and premature death but protects mice from aggressive liver cancer. Hepatology. 2012; 55:941–952. [PubMed: 22031092]
47. Cui Y, Hosui A, Sun R, et al. Loss of signal transducer and activator of transcription 5 leads to hepatosteatosis and impaired liver regeneration. Hepatology. 2007; 46:504–513. [PubMed: 17640041]
48. Debeljuk L, Steger RW, Wright JC, Mattison J, Bartke A. Effects of overexpression of growth hormone-releasing hormone on the hypothalamo-pituitary-gonadal function in the mouse. Endocrine. 1999; 11:171–179. [PubMed: 10709765]
49. Moride Y, Hayes JF. Correlated responses in growth hormone to selection for weight gain in mice. J Anim Breed Genet. 1993; 110:450–458. [PubMed: 21395743]
50. Poole TM, Drinkwater NR. Hormonal and genetic interactions in murine hepatocarcinogenesis. Prog Clin Biol Res. 1995; 391:187–194. [PubMed: 8532716]
51. Waxman DJ, O'Connor C. Growth hormone regulation of sex-dependent liver gene expression. Mol Endocrinol. 2006; 20:2613–2629. [PubMed: 16543404]
52. Yang JD, Roberts LR. Hepatocellular carcinoma: A global view. Nat Rev Gastroenterol Hepatol. 2010; 7:448–458. [PubMed: 20628345]
53. Hanahan D, Weinberg RA. The hallmarks of cancer. Cell. 2000; 100:57–70. [PubMed: 10647931]
54. Griffin AC, Richardson HL, Robertson CH, O'Neal MA, Spain JD. The role of hormones in liver carcinogenesis. J Natl Cancer Inst. 1955; 15:1623–1632. [PubMed: 13243105]
55. Griffin AC, Rinfret AP, Corsiglia VF. The inhibition of liver carcinogenesis with 3′-methyl-4-dimethylaminoazobenzene in hypophysectomized rats. Cancer Res. 1953; 13:77–79. [PubMed: 13032954]

56. Richardson HL, Griffin AC, Rinfret AP. Adrenal histological change and liver-tumor inhibition in hypophysectomized rats fed the azo dye, 3′-methyl-4-dimethylaminoazobenzene. Cancer. 1953; 6:1025–1029. [PubMed: 13094651]

57. Robertson CH, O'Neal MA, Richardson HL, Griffin AC. Further observations on the role of the pituitary and the adrenal gland in azo dye carcinogenesis. Cancer Res. 1954; 14:549–553. [PubMed: 13199795]

58. Cui Y, Riedlinger G, Miyoshi K, et al. Inactivation of Stat5 in mouse mammary epithelium during pregnancy reveals distinct functions in cell proliferation, survival, and differentiation. Mol Cell Biol. 2004; 24:8037–8047. [PubMed: 15340066]

59. Threadgill DW, Dlugosz AA, Hansen LA, et al. Targeted disruption of mouse EGF receptor: effect of genetic background on mutant phenotype. Science. 1995; 269:230–234. [PubMed: 7618084]

60. Abbas T, Dutta A. p21 in cancer: intricate networks and multiple activities. Nat Rev Cancer. 2009; 9(6):400–414. [PubMed: 19440234]

61. To MD, Perez-Losada J, Mao J-H, Hsu J, Jacks T, Balmain A. A functional switch from lung cancer resistance to susceptibility at the Pas1 locus in Kras2LA2 mice. Nat Genet. 2006; 38:926–930. [PubMed: 16823377]

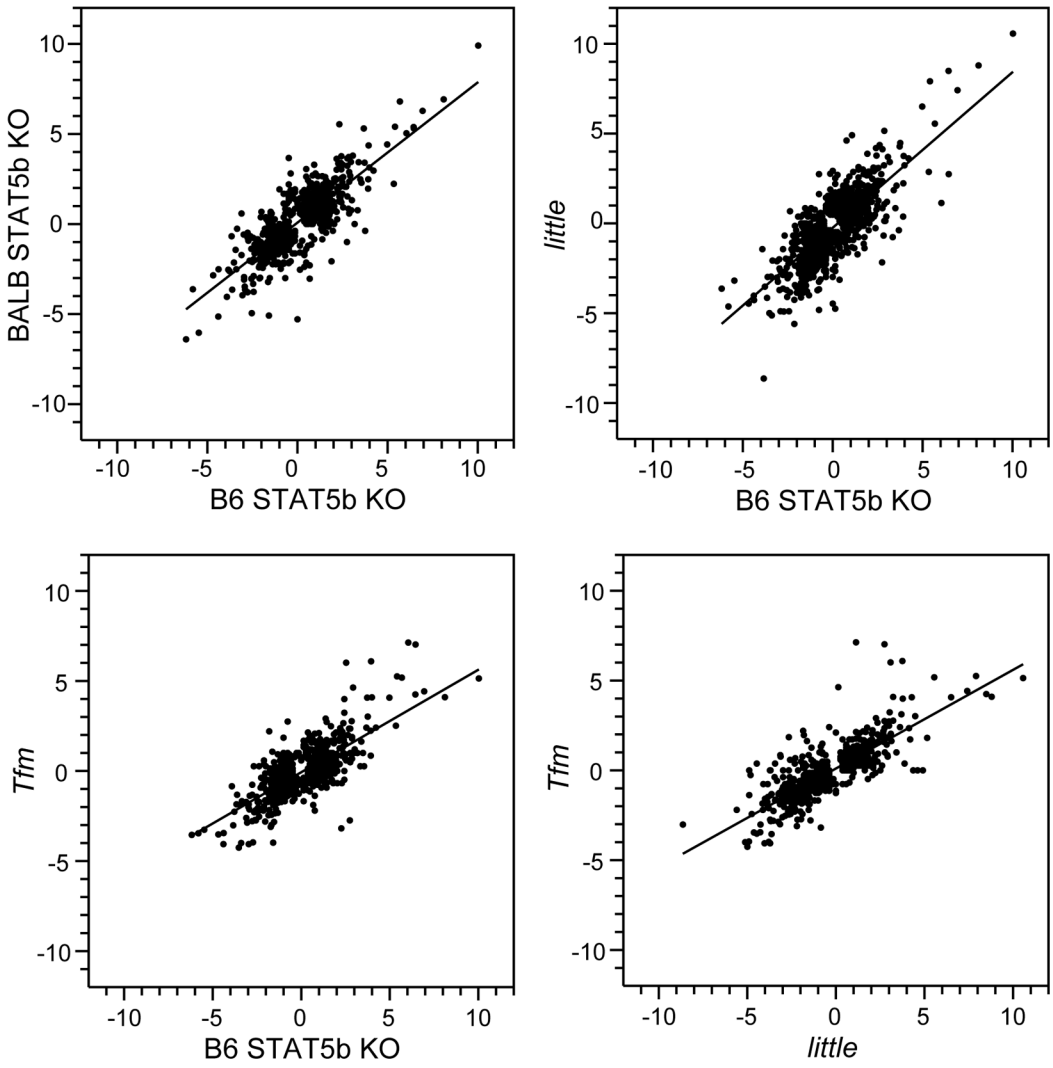

Figure 1.

Pairwise analysis of differential gene expression. In each plot, the X and Y axes are the $\log_2$ fold-change for the indicated strain relative to wild-type for every gene with FDR < 0.01 in either strain.

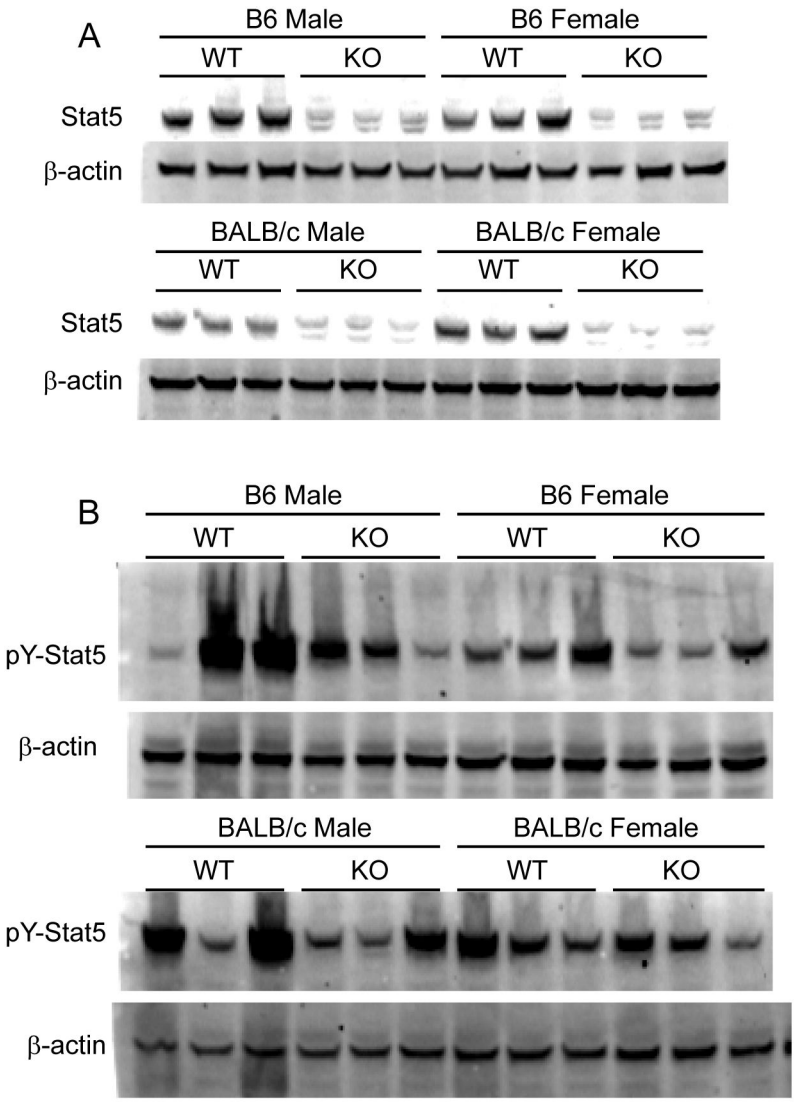

Figure 2.

STAT5 expression in the liver. A) Western blot analysis of total STAT5 (STAT5a and STAT5b) protein in liver lysates from 10-week-old mice. β-Actin was used as a loading control. B) Western blot analysis of tyrosine-phosphorylated (Tyr694) STAT5 (pY-STAT5) proteins in liver lysates from 10-week-old mice. β-Actin was used as a loading control.

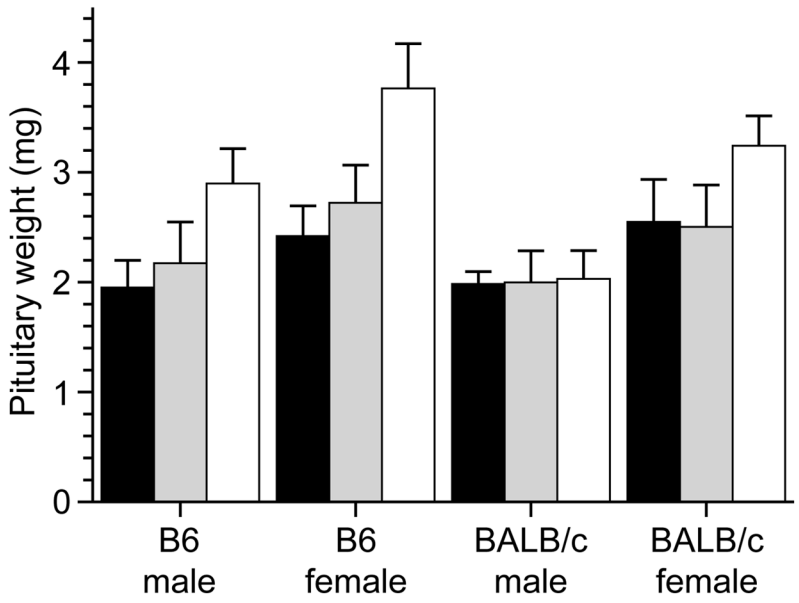

Figure 3.

Average mass of pituitaries isolated from 10-week-old C57BL/6J and BALB/cJ STAT5b KO congenics. For each strain/sex, the color of the bar indicates the genotype: black, wild-type; gray, heterozygote; white, homozygous mutant. The numbers of mice per group (wild-type, heterozygote, KO) were: B6 male 14, 12, 15; B6 female 17, 10, 14; BALB/c male 11, 13, 6; BALB/c female 15, 12, 9.

Table 1

Genes differentially expressed in mutants relative to the corresponding wild-type strain.

	Number DE genes[a]		Spearman correlation coeff. (P-value)[b]		
Strain	**Down**	**Up**	**BALB *Stat5b*$^{-/-}$**	***little***	***Tfm***
B6 *Stat5b*$^{-/-}$	294	318	0.77 (10^{-108})	0.70 (10^{-121})	0.64 (10^{-65})
BALB *Stat5b*$^{-/-}$	179	250		0.70 (10^{-107})	0.68 (10^{-57})
little	450	296			0.80 (10^{-115})
Tfm	129	102			

[a] Liver RNA was hybridized to a mouse whole-genome Agilent microarray. Numbers reflect genes that were expressed at levels significantly different (FDR < 0.01) from those in the corresponding wild-type strain.

[b] Inter-strain correlations in the $\log_2$ (fold-change) relative to wild-type for all genes that were differentially expressed (FDR < 0.01) in either strain were determined by the Spearman rank correlation test.

Table 2

Top ten transcription factors for the DE genes in each experimental group.

Transcription factor gene	*P*-value[a]			
	***Tfm*/Y**	***little***	**B6 STAT5b KO**	**BALB/c STAT5b KO**
Rorc	5.0×10^{-24}	4.7×10^{-22}	2.6×10^{-21}	3.1×10^{-26}
Rora	6.6×10^{-22}	1.9×10^{-21}	1.6×10^{-21}	1.2×10^{-27}
Ppara	1.4×10^{-08}	4.0×10^{-07}	4.0×10^{-14}	2.4×10^{-11}
Stat5b	2.3×10^{-08}	8.0×10^{-06}	2.4×10^{-02}	3.5×10^{-03}
Nr1i2	8.3×10^{-08}	9.1×10^{-09}	8.3×10^{-09}	2.4×10^{-11}
Nr1i3	1.7×10^{-07}	3.8×10^{-11}	4.0×10^{-06}	3.2×10^{-09}
Ahr	2.4×10^{-06}	3.2×10^{-06}	3.0×10^{-05}	1.2×10^{-06}
Med1	4.5×10^{-04}	6.2×10^{-03}	9.2×10^{-05}	5.0×10^{-07}
Ar	4.8×10^{-02}	2.2×10^{-02}	7.2×10^{-03}	4.8×10^{-03}
Rxra	8.2×10^{-03}	4.0×10^{-02}	7.9×10^{-03}	1.1×10^{-04}

[a]The significance of the overlap between sets of differentially expressed genes and those predicted to be regulated by specific transcription factors was determined using Fisher's exact test.

Table 3

Hepatocarcinogenesis in STAT5b KO congenic mice.

Background	Sex	*Stat5b* genotype[a]	Num. mice	Mean tumor multiplicity[b]	Tumors >5 mm[c]
BALB/cJ N_{11}	M	WT	14	7.6 ± 5.9	0
		Het	43	3.4 ± 4.5[d]	0.02 ± 0.15
		KO	15	10 ± 11	0
BALB/cJ N_{11}	F	WT	29	12 ± 12	0.17 ± 0.47
		Het	36	13 ± 17	0.03 ± 0.17
		KO	24	11 ± 10	0.21 ± 0.41
C57BL/6J N_6	M	WT	32	22 ± 20	0.6 ± 1
		Het	49	27 ± 23	0.8 ± 2
		KO	32	52 ± 38[e]	3.2 ± 4.1[e]
C57BL/6J N_6	F	WT	33	17 ± 20	0.6 ± 2
		Het	41	18 ± 14	0.9 ± 2
		KO	25	40 ± 25[d]	2.6 ± 4.2[e]
C3H/HeJ N_6	M	WT	14	136 ± 63	3.3 ± 3.9
		Het	25	111 ± 47	6.1 ± 5.4
		KO	5	51 ± 28[d]	0.40 ± 0.55
C3H/HeJ N_6	F	WT	6	59 ± 19	1.2 ± 0.8
		Het	17	49 ± 26	0.8 ± 1.5
		KO	5	10 ± 9[d]	0.2 ± 0.4

[a] Genotypes: WT, +/+; Het, +/−; KO, −/−.

[b] Male mice aged 32 weeks and female mice aged 50 weeks before sacrifice.

[c] Mean number of tumors > 5 mm per animal.

[d] $P < 0.05$ relative to wild-type.

[e] $P < 0.01$ relative to wild-type.

$^{f}P < 0.001$ relative to wild-type.